Science Advances
AAAS

Supplementary Materials for

Functional anatomy of the subthalamic nucleus and the pathophysiology of cardinal features of Parkinson's disease unraveled by focused ultrasound ablation

Rafael Rodriguez-Rojas *et al.*

Corresponding author: José A. Obeso, jobeso.hmcinac@hmhospitales.com

Sci. Adv. **10**, eadr9891 (2024)
DOI: 10.1126/sciadv.adr9891

The PDF file includes:

Figs. S1 to S5
Tables S1 and S2
Legends for data S1 and S2
References

Other Supplementary Material for this manuscript includes the following:

Data S1 and S2

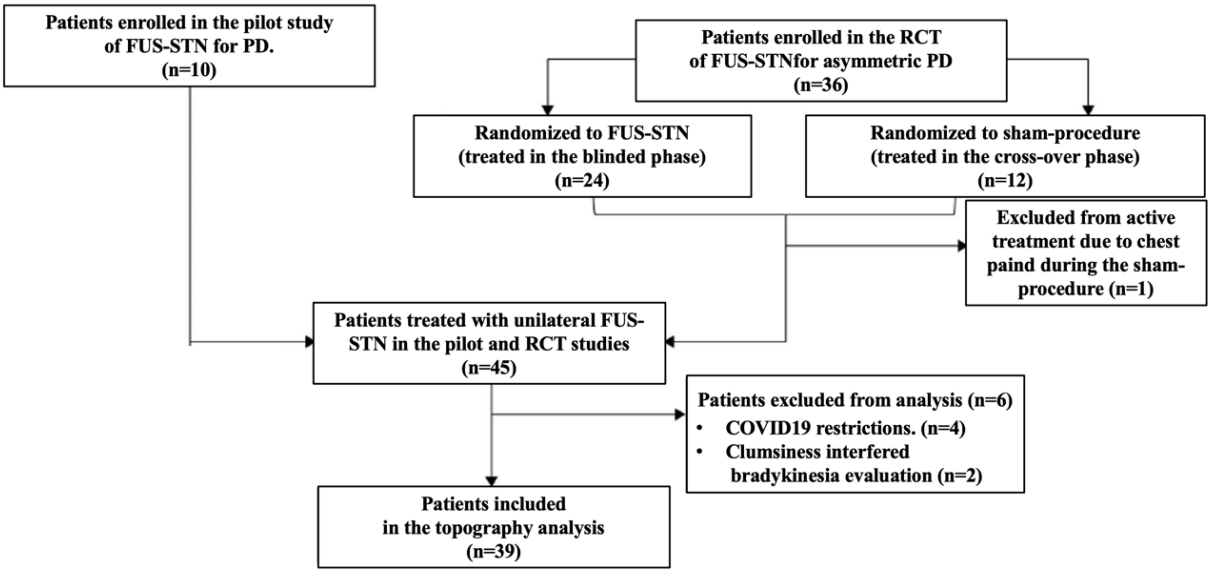

Fig. S1.

Patients treated with unilateral FUS-STN included in the topographic analysis.

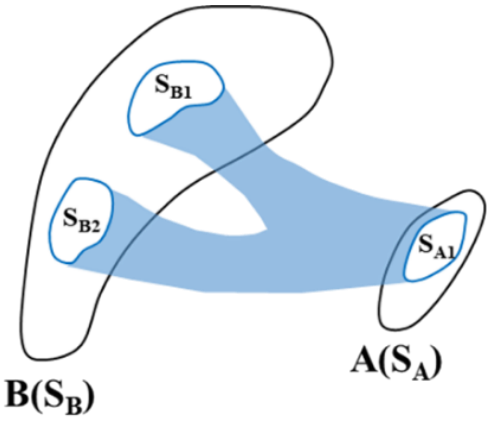

$$ACD_{A,B} = \frac{S_{A1}}{S_A} + \frac{S_{B1} + S_{B2}}{S_B}$$

Fig. S2.

The anatomical connection density. The ACD measure (75) is the ratio between the "effective" number of voxels over the surface of both regions, weighting each voxel by its connectivity value with the connected region, and the total number of considered superficial voxels. Thus, for any subject and pair of regions i and j, the ACDi,j measure ($0 \leq ACD_{i;j} \leq 1$; $ACD_{i,j} \equiv ACD_{ji}$) reflects the fraction of the region's surface involved in the axonal connection with respect to the total surface of both regions. In this way, ACD reflects the degree of evidence supporting the existence of each connection, after controlling for the size of the region. For each motor feature, we calculated its anatomical connectivity pattern as the ACD matrix between the 'significant mean effect image' and six regions defined by a human motor area template.

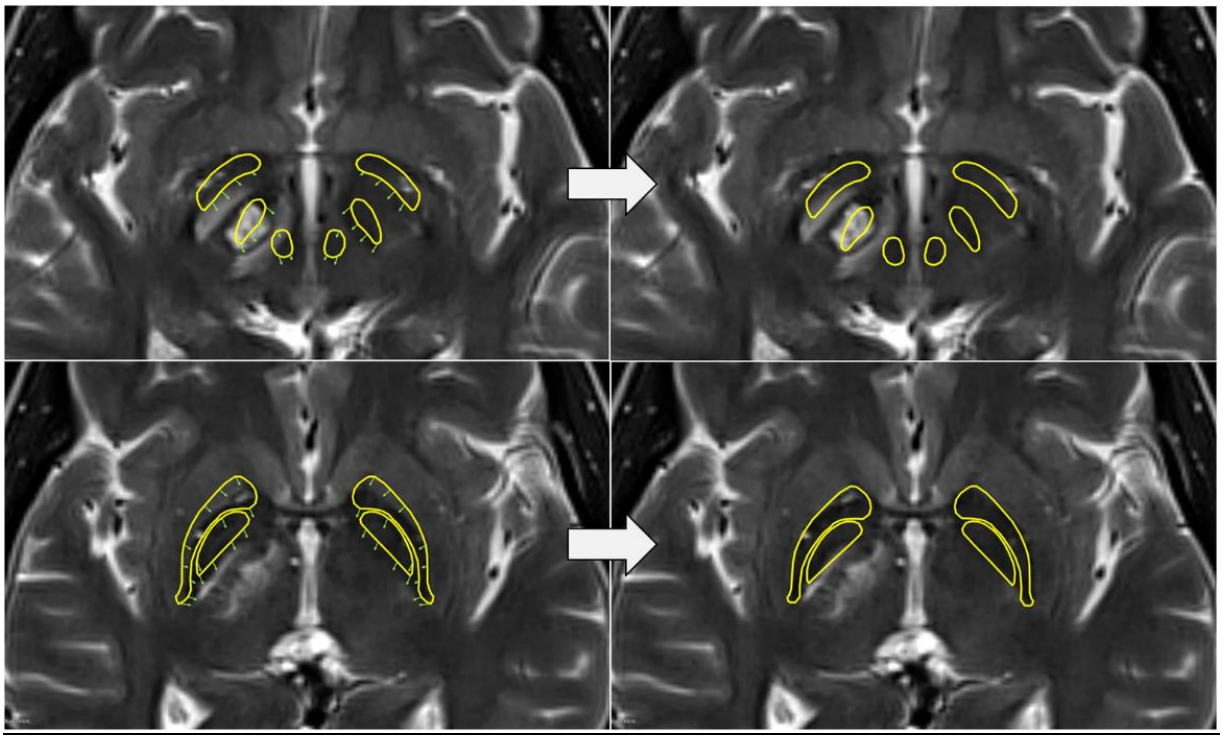

Fig. S3.

Manual refinement using 3DSlicer. Example T2 slices (fast spin echo, pixel size = 0.5mm, slice thickness = 2mm) acquired 24 hours after FUS-subthalamotomy. Yellow outlines feature DISTAL atlas structures after automated registration into MNI space with SPM12 (78). Note the mismatch between outlines and underlying anatomical structures. Affine manual refinement of deformation fields accounted for these differences.

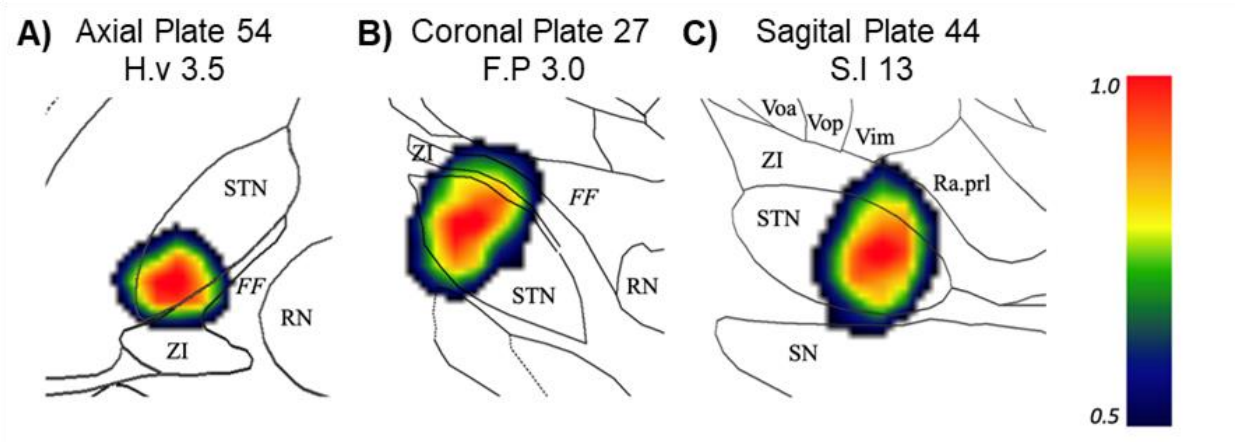

Fig. S4.

Probabilistic FUS lesion maps (N-image, all subjects) respective to the Schaltenbrand and Wahren atlas (79). (A) Axial slice at 3-4 mm under the commissural plane, (B) Coronal slice at 3 mm posterior to the inter-commissural point, (C) Sagittal slice at 13 mm lateral to midline. (STN: subthalamic nucleus). On average, the center of the lesion was well within the motor region of the STN. ZI: zona incerta; RN: red nucleus; FF: fields of Forel; SN: subtantia nigra; Voa/Vop: ventralis oralis anterior/posterior nuclei of the thalamus; Vim: ventralis intermedius nucleus of the thalamus; Ra.prl prelemniscal radiation).

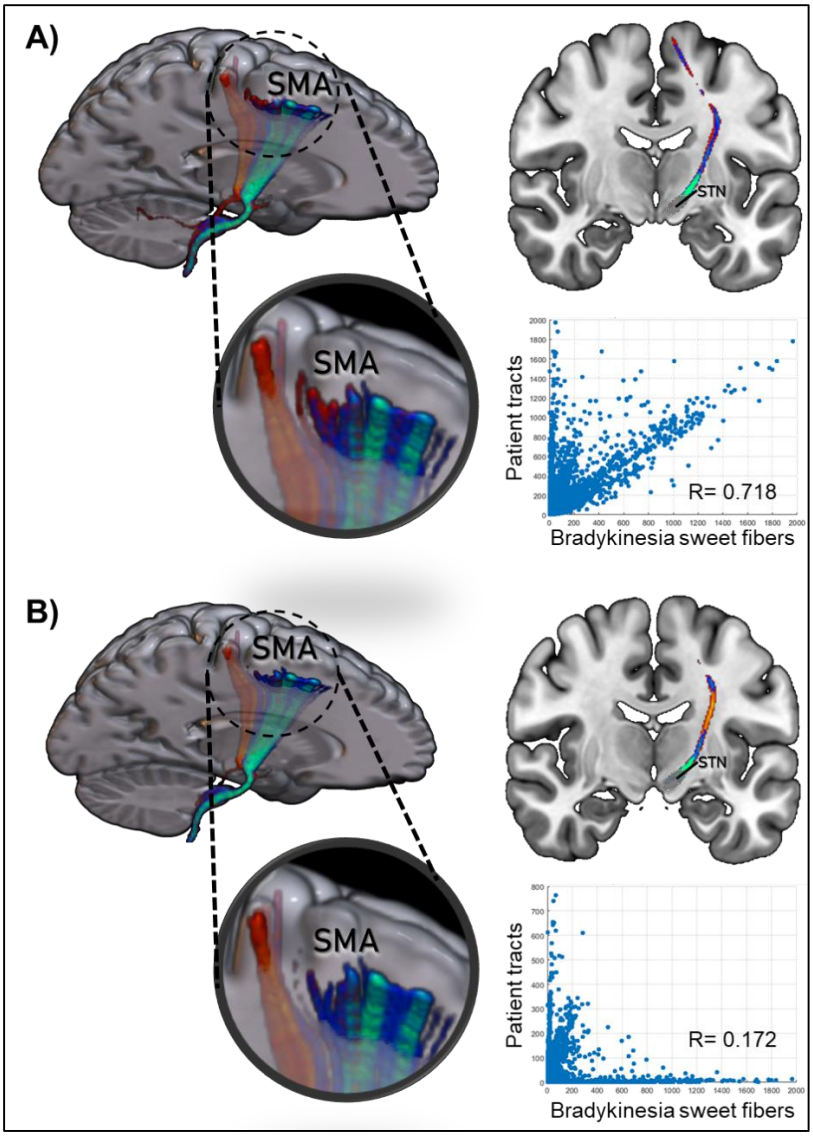

Fig. S5.

Example of prediction based on fiber tract impact. Prediction of treatment-induced improvement in bradykinesia is shown for two extreme example patients. In both cases the patients's streamlines (streamlines distribution seeding from lesion, in hot colors) and sweet fibers (streamlines seeding from bradykinesia sweetspot, in winter colors) are rendered in the MNI template (left panels). SMA region is zoomed to facilitate visual inspection. Tract density images superimposed in MNI template are shown in top right panel. Spatial correlations are shown in scatter plots (right bottom panel), where blue dots represent voxels where density values of effective streamlines are different from 0. A) Example patient with strong overlap of his lesioned tract with sweet fibers significantly improved in bradykinesia score (% improvement = 100%, Patient 36, Data S2). B) Patient with less overlap received a lower improvement in bradykinesia score (% improvement = 16.7%, Patient 5, Data S2). Note the scarcity of patient's connections (hot colors) in SMA, as well as areas of poor overlap in the course of the tracts. Of note, several voxels barely overlapped with the sweet tract and consequently received a near-zero score (scatter plot).

	Volume (mm^3)				
Sweet-spot:	Total	M1	SMA	Associative	Limbic
Bradykinesia	34.9	5.5	26.8	2.6	0.0
Rigidity	10.9	2.9	7.9	0.1	0.0
Tremor	15.9	10.8	5.1	0.0	0.0

Table S1.
Estimated volumes of significant mean effect maps impacting in subthalamic subregions.

Region*	**$V_{SMA-STN}$**	**V_{M1-STN}**	**$V_{Assoc-STN}$**	**$V_{Limbic-STN}$**
Volume ± s.d. (mm^3) §	31.47 ± 16.3	20.91 ± 9.7	9.1 ± 6.6	0.13 ± 0.7
Bradykinesia				
t-value	**5.322**	-0.031	-0.003	0.636
Partial R	**0.658**	-0.005	0.000	0.105
p-value	**<0.001**	0.975	0.998	0.529
Rigidity				
t-value	**2.971**	1.533	1.451	0.990
Partial R	**0.439**	0.248	0.235	0.163
p-value	**0.005**	0.134	0.155	0.329
Tremor				
t-value	1.409	**2.657**	0.725	0.591
Partial R	0.245	**0.425**	0.129	0.106
p-value	0.169	**0.012**	0.474	0.559

Table S2.

Stepwise multiple regression analysis to account for the relationship between lesion topography and the functional organization of the STN. Variables included in the final statistical model are shown in bold.

*Atlas-based subthalamic regions defined by the connectivity with functionally relevant cortical regions (6).

§ Overlap volume between patient's lesions and atlas-defined STN sub-regions.

Data S1. Morphometric values (separate file 'Data_S1.xlsx')

Each row represents a subject included in the study (n=39). The table shows volume (mm^3) of the overall lesion (V_{TOT}). and the impact on the subthalamic nucleus (V_{STN}). and the SMA-STN. M1-STN associative and limbic respective sub-regions according to the 24h post-treatment MRI. Coordinates of the center of mass of the lesion within the STN are shown both according to MNI system and with respect to ACPC. X represents the latero-medial axis coordinate; thus larger positive values indicate more lateral with respect to midline. Y represents the rostro-caudal axis coordinate; thus larger positive values indicate more distance posterior with respect to mid-commisural point. Z represents the dorso-ventral axis coordinate; thus larger positive values indicate more ventral distance with respect to the ACPC plane.

Data S2. Clinical outcome. (separate file 'Data_S2.xlsx')

Each row represents a subject included in the study (n=39). The table shows motor outcomes for every patient. Left columns show scores for the treated side (i.e.. most affected side) at baseline. Motor outcomes are presented as "% of change" in the respective MDS-UPDRS-III sub scores. Contralateral score for rigidity (item 3.3. unilateral assessment includes evaluation of rigidity in the upper and lower limbs and ranges from 0 to 8 with higher scores indicating greater rigidity). bradykinesia (items 3.4 – 3.8. unilateral assessment includes evaluation of the upper and lower limb and ranges from 0 to 20. with higher scores indicating greater bradykinesia) and resting tremor (items 3.17. unilateral assessment includes evaluation of rest tremor in the upper and lower limbs ranging from 0 to 8. Higher scores indicate worst motor condition.

% of change= [(score at baseline - score at last follow up)/baseline score] * 100

with higher positive values meaning larger improvement. NA=not applicable (for tremor improvement in patients without resting tremor at baseline).

REFERENCES AND NOTES

1. M. R. DeLong, T. Wichmann, Basal ganglia circuits as targets for neuromodulation in Parkinson disease. *JAMA Neurol.* **72**, 1354–1360 (2015).

2. P. Krack, J. Volkmann, G. Tinkhauser, G. Deuschl, Deep brain stimulation in movement disorders: From experimental surgery to evidence-based therapy. *Mov. Disord.* **34**, 1795–1810 (2019).

3. W. I. Haynes, S. N. Haber, The organization of prefrontal-subthalamic inputs in primates provides an anatomical substrate for both functional specificity and integration: Implications for Basal Ganglia models and deep brain stimulation. *J. Neurosci.* **33**, 4804–4814 (2013).

4. M. C. Keuken, H. B. M. Uylings, S. Geyer, A. Schäfer, R. Turner, B. U. Forstmann, Are there three subdivisions in the primate subthalamic nucleus? *Front Neuroanat.* **6**, 14 (2012).

5. A. Nambu, M. Takada, M. Inase, H. Tokuno, Dual somatotopical representations in the primate subthalamic nucleus: Evidence for ordered but reversed body-map transformations from the primary motor cortex and the supplementary motor area. *J. Neurosci.* **16**, 2671–2683 (1996).

6. H. Iwamuro, Y. Tachibana, Y. Ugawa, N. Saito, A. Nambu, Information processing from the motor cortices to the subthalamic nucleus and globus pallidus and their somatotopic organizations revealed electrophysiologically in monkeys. *Eur. J. Neurosci.* **46**, 2684–2701 (2017).

7. R. Rodriguez-Rojas, J. A. Pineda-Pardo, J. Manez-Miro, A. Sanchez-Turel, R. Martinez-Fernandez, M. Del Alamo, M. DeLong, J. A. Obeso, Functional topography of the human subthalamic nucleus: Relevance for subthalamotomy in Parkinson's disease. *Mov. Disord.* **37**, 279–290 (2022).

8. C. D. Marsden, The mysterious motor function of the basal ganglia: The Robert Wartenberg Lecture. *Neurology* **32**, 514–539 (1982).

9. P. Redgrave, M. Rodriguez, Y. Smith, M. C. Rodriguez-Oroz, S. Lehericy, H. Bergman, Y. Agid, M. R. DeLong, J. A. Obeso, Goal-directed and habitual control in the basal ganglia: Implications for Parkinson's disease. *Nat. Rev. Neurosci.* **11**, 760–772 (2010).

10. J. A. Obeso, M. Jahanshahi, L. Alvarez, R. Macias, I. Pedroso, L. Wilkinson, N. Pavon, B. Day, S. Pinto, M. C. Rodríguez-Oroz, J. Tejeiro, J. Artieda, P. Talelli, O. Swayne, R. Rodríguez, K. Bhatia, M. Rodriguez-Diaz, G. Lopez, J. Guridi, J. C. Rothwell, What can man do without basal ganglia motor output? The effect of combined unilateral subthalamotomy and pallidotomy in a patient with Parkinson's disease. *Exp. Neurol.* **220**, 283–292 (2009).

11. H. Narabayashi, T. Okuma, S. Shikiba, Procaine oil blocking of the globus pallidus. *AMA Arch Neurol. Psychiatry* **75**, 36–48 (1956).

12. R. Hassler, T. Riechert, F. Mundinger, W. Umbach, J. A. Ganglberger, Physiological observations in stereotaxic operations in extrapyramidal motor disturbances. *Brain* **83**, 337–350 (1960).

13. H. Narabayashi, "Muscle tone conducting system and tremor concerned structures" in *Third Symposium on Parkinson's Disease*, F. J. Gillingham, I. M. L. Donaldson, Eds. (Livingstone, 1969), pp. 246–251.

14. A. Horn, W. J. Neumann, K. Degen, G. H. Schneider, A. A. Kühn, Toward an electrophysiological "sweet spot" for deep brain stimulation in the subthalamic nucleus. *Hum. Brain Mapp.* **38**, 3377–3390 (2017).

15. H. Akram, S. N. Sotiropoulos, S. Jbabdi, D. Georgiev, P. Mahlknecht, J. Hyam, T. Foltynie, P. Limousin, E. De Vita, M. Jahanshahi, M. Hariz, J. Ashburner, T. Behrens, L. Zrinzo, Subthalamic deep brain stimulation sweet spots and hyperdirect cortical connectivity in Parkinson's disease. *Neuroimage* **158**, 332–345 (2017).

16. T. A. Dembek, J. Roediger, A. Horn, P. Reker, C. Oehrn, H. S. Dafsari, N. Li, A. A. Kühn, G. R. Fink, V. Visser-Vandewalle, M. T. Barbe, L. Timmermann, Probabilistic sweet spots

predict motor outcome for deep brain stimulation in Parkinson disease. *Ann. Neurol.* **86**, 527–538 (2019).

17. R. Verhagen, L. J. Bour, V. J. J. Odekerken, P. van den Munckhof, P. R. Schuurman, R. M. A. de Bie, Electrode location in a microelectrode recording-based model of the subthalamic nucleus can predict motor improvement after deep brain stimulation for Parkinson's disease. *Brain Sci.* **9**, 51 (2019).

18. N. Rajamani, H. Friedrich, K. Butenko, T. Dembek, F. Lange, P. Navrátil, P. Zvarova, B. Hollunder, R. M. A. de Bie, V. J. J. Odekerken, J. Volkmann, X. Xu, Z. Ling, C. Yao, P. Ritter, W. J. Neumann, G. P. Skandalakis, S. Komaitis, A. Kalyvas, C. Koutsarnakis, G. Stranjalis, M. Barbe, V. Milanese, M. D. Fox, A. A. Kühn, E. Middlebrooks, N. Li, M. Reich, C. Neudorfer, A. Horn, Deep brain stimulation of symptom-specific networks in Parkinson's disease. *Nat. Commun.* **15**, 4662 (2024).

19. P. Krack, R. Martinez-Fernandez, M. Del Alamo, J. A. Obeso, Current applications and limitations of surgical treatments for movement disorders. *Mov. Disord.* **32**, 36–52 (2017).

20. R. C. Helmich, The cerebral basis of Parkinsonian tremor: A network perspective. *Mov. Disord.* **33**, 219–231 (2018).

21. W. J. Neumann, L. A. Steiner, L. Milosevic, Neurophysiological mechanisms of deep brain stimulation across spatiotemporal resolutions. *Brain* **146**, 4456–4468 (2023).

22. T. Wichmann, H. Bergman, M. R. DeLong, The primate subthalamic nucleus. III. Changes in motor behavior and neuronal activity in the internal pallidum induced by subthalamic inactivation in the MPTP model of parkinsonism. *J. Neurophysiol.* **72**, 521–530 (1994).

23. J. Guridi, M. R. Luquin, M. T. Herrero, J. A. Obeso, The subthalamic nucleus: A possible target for stereotaxic surgery in Parkinson's disease. *Mov. Disord.* **8**, 421–429 (1993).

24. E. Bates, S. M. Wilson, A. P. Saygin, F. Dick, M. I. Sereno, R. T. Knight, N. F. Dronkers, Voxel-based lesion-symptom mapping. *Nat. Neurosci.* **6**, 448–450 (2003).

25. R. Martinez-Fernandez, R. Rodriguez-Rojas, M. Del Álamo, F. Hernandez-Fernandez, J. A. Pineda-Pardo, M. Dileone, F. Alonso-Frech, G. Foffani, I. Obeso, C. Gasca-Salas, E. de Luis-Pastor, L. Vela, J. A. Obeso, Focused ultrasound subthalamotomy in patients with asymmetric Parkinson's disease: A pilot study. *Lancet Neurol.* **17**, 54–63 (2018).

26. R. Martínez-Fernández, J. U. Máñez-Miró, R. Rodríguez-Rojas, M. Del Álamo, B. B. Shah, F. Hernández-Fernández, J. A. Pineda-Pardo, M. H. G. Monje, B. Fernández-Rodríguez, S. A. Sperling, D. Mata-Marín, P. Guida, F. Alonso-Frech, I. Obeso, C. Gasca-Salas, L. Vela-Desojo, W. J. Elias, J. A. Obeso, Randomized trial of focused ultrasound subthalamotomy for Parkinson's disease. *N. Engl. J. Med.* **383**, 2501–2513 (2020).

27. R. Martínez Fernández, E. Natera Villalba, R. Rodríguez-Rojas, M. Del Álamo, J. A. Pineda-Pardo, I. Obeso, D. Mata-Marín, P. Guida, T. Jimenez-Castellanos, D. Pérez-Bueno, A. Duque, J. U. Máñez Miró, C. Gasca-Salas, M. Matarazzo, J. A. Obeso, Unilateral focused ultrasound subthalamotomy in early Parkinson's disease: A pilot study. *J. Neurol. Neurosurg. Psychiatry* **95**, 206–213 (2024).

28. M. A. Mayka, D. M. Corcos, S. E. Leurgans, D. E. Vaillancourt, Three-dimensional locations and boundaries of motor and premotor cortices as defined by functional brain imaging: A meta-analysis. *Neuroimage* **31**, 1453–1474 (2006).

29. F. C. Yeh, Population-based tract-to-region connectome of the human brain and its hierarchical topology. *Nat. Commun.* **13**, 4933 (2022).

30. W. Penfield, B. Milner, Memory deficit produced by bilateral lesions in the hippocampal zone. *AMA Arch. Neurol. Psychiatry* **79**, 475–497 (1958).

31. J. Joutsa, N. Lipsman, A. Horn, G. R. Cosgrove, M. D. Fox, The return of the lesion for localization and therapy. *Brain* **146**, 3146–3155 (2023).

32. P. Cintas, M. Simonetta-Moreau, F. Ory, C. Brefel-Courbon, N. Fabre, P. Chaynes, J. Sabatier, J. C. Sol, O. Rascol, I. Berry, Y. Lazorthes, Deep brain stimulation for Parkinson's disease: Correlation between intraoperative subthalamic nucleus neurophysiology and most effective contacts. *Stereotact. Funct. Neurosurg.* **80**, 108–113 (2003).

33. B. Hollunder, J. L. Ostrem, I. A. Sahin, N. Rajamani, S. Oxenford, K. Butenko, C. Neudorfer, P. Reinhardt, P. Zvarova, M. Polosan, H. Akram, M. Vissani, C. Zhang, B. Sun, P. Navratil, M. M. Reich, J. Volkmann, F. C. Yeh, J. C. Baldermann, T. A. Dembek, V. Visser-Vandewalle, E. J. L. Alho, P. R. Franceschini, P. Nanda, C. Finke, A. A. Kühn, D. D. Dougherty, R. M. Richardson, H. Bergman, M. R. DeLong, A. Mazzoni, L. M. Romito, H. Tyagi, L. Zrinzo, E. M. Joyce, S. Chabardes, P. A. Starr, N. Li, A. Horn, Mapping dysfunctional circuits in the frontal cortex using deep brain stimulation. *Nat. Neurosci.* **27**, 573–586 (2024).

34. G. E. Alexander, M. R. DeLong, P. L. Strick, Parallel organization of functionally segregated circuits linking basal ganglia and cortex. *Annu. Rev. Neurosci.* **9**, 357–381 (1986).

35. A. Nambu, H. Tokuno, M. Inase, M. Takada, Corticosubthalamic input zones from forelimb representations of the dorsal and ventral divisions of the premotor cortex in the macaque monkey: Comparison with the input zones from the primary motor cortex and the supplementary motor area. *Neurosci. Lett.* **239**, 13–16 (1997).

36. M. Takada, H. Tokuno, A. Nambu, M. Inase, Corticostriatal projections from the somatic motor areas of the frontal cortex in the macaque monkey: Segregation versus overlap of input zones from the primary motor cortex, the supplementary motor area, and the premotor cortex. *Exp. Brain Res.* **120**, 114–128 (1998).

37. S. Rahimpour, S. Rajkumar, M. Hallett, The supplementary motor complex in Parkinson's disease. *J. Mov. Disord.* **15**, 21–32 (2022).

38. E. D. Playford, I. H. Jenkins, R. E. Passingham, J. Nutt, R. S. Frackowiak, D. J. Brooks, Impaired mesial frontal and putamen activation in Parkinson's disease: A positron emission tomography study. *Ann. Neurol.* **32**, 151–161 (1992).

39. U. Sabatini, K. Boulanouar, N. Fabre, F. Martin, C. Carel, C. Colonnese, L. Bozzao, I. Berry, J. L. Montastruc, F. Chollet, O. Rascol, Cortical motor reorganization in akinetic patients with Parkinson's disease: A functional MRI study. *Brain* **123**, 394–403 (2000).

40. T. Wu, M. Hallett, A functional MRI study of automatic movements in patients with Parkinson's disease. *Brain* **128**, 2250–2259 (2005).

41. G. E. Alexander, M. D. Crutcher, Preparation for movement: Neural representations of intended direction in three motor areas of the monkey. *J. Neurophysiol.* **64**, 133–150 (1990).

42. M. Jahanshahi, I. H. Jenkins, R. G. Brown, C. D. Marsden, R. E. Passingham, D. J. Brooks, Self-initiated versus externally triggered movements. I. An investigation using measurement of regional cerebral blood flow with PET and movement-related potentials in normal and Parkinson's disease subjects. *Brain* **118**, 913–933 (1995).

43. T. Ninomiya, K. I. Inoue, E. Hoshi, M. Takada, Layer specificity of inputs from supplementary motor area and dorsal premotor cortex to primary motor cortex in macaque monkeys. *Sci. Rep.* **9**, 18230 (2019).

44. M. Bologna, G. Paparella, A. Fasano, M. Hallett, A. Berardelli, Evolving concepts on bradykinesia. *Brain* **143**, 727–750 (2020).

45. A. Nambu, S. Chiken, H. Sano, N. Hatanaka, J. A. Obeso, Dynamic activity model of movement disorders: The fundamental role of the hyperdirect pathway. *Mov. Disord.* **38**, 2145–2150 (2023).

46. R. Chen, A. Berardelli, A. Bhattacharya, M. Bologna, K. S. Chen, A. Fasano, R. C. Helmich, W. D. Hutchison, N. Kamble, A. A. Kühn, A. Macerollo, W.-J. Neumann, P. K. Pal, G. Paparella, A. Suppa, K. Udupa, Clinical neurophysiology of Parkinson's disease and parkinsonism. *Clin. Neurophysiol. Pract.* **7**, 201–227 (2022).

47. N. Baradaran, S. N. Tan, A. Liu, A. Ashoori, S. J. Palmer, Z. J. Wang, M. M. K. Oishi, M. J. McKeown, Parkinson's disease rigidity: Relation to brain connectivity and motor performance. *Front. Neurol.* **4**, 67 (2013).

48. H. T. Benamer, W. H. Oertel, J. Patterson, D. M. Hadley, O. Pogarell, H. Höffken, A. Gerstner, D. G. Grosset, Prospective study of presynaptic dopaminergic imaging in patients with mild Parkinsonism and tremor disorders: Part 1. Baseline and 3-month observations. *Mov. Disord.* **18**, 977–984 (2003).

49. S. A. Shimamoto, E. S. Ryapolova-Webb, J. L. Ostrem, N. B. Galifianakis, K. J. Miller, P. A. Starr, Subthalamic nucleus neurons are synchronized to primary motor cortex local field potentials in Parkinson's disease. *J. Neurosci.* **33**, 7220–7233 (2013).

50. V. Raos, G. Franchi, V. Gallese, L. Fogassi, Somatotopic organization of the lateral part of area F2 (dorsal premotor cortex) of the macaque monkey. *J. Neurophysiol.* **89**, 1503–1518 (2003).

51. D. Akkal, R. P. Dum, P. L. Strick, Supplementary motor area and presupplementary motor area: Targets of basal ganglia and cerebellar output. *J. Neurosci.* **27**, 10659–10673 (2007).

52. A. C. Bostan, R. P. Dum, P. L. Strick, Cerebellar networks with the cerebral cortex and basal ganglia. *Trends Cogn. Sci.* **17**, 241–254 (2013).

53. H. Mure, S. Hirano, C. C. Tang, I. U. Isaias, A. Antonini, Y. Ma, V. Dhawan, D. Eidelberg, Parkinson's disease tremor-related metabolic network: Characterization, progression, and treatment effects. *Neuroimage* **54**, 1244–1253 (2011).

54. A. Quartarone, A. Cacciola, D. Milardi, M. F. Ghilardi, A. Calamuneri, G. Chillemi, G. Anastasi, J. Rothwell, New insights into cortico-basal-cerebellar connectome: Clinical and physiological considerations. *Brain* **143**, 396–406 (2020).

55. A. C. Bostan, R. P. Dum, P. L. Strick, The basal ganglia communicate with the cerebellum. *Proc. Natl. Acad. Sci. U.S.A.* **107**, 8452–8456 (2010).

56. R. C. Helmich, M. J. Janssen, W. J. Oyen, B. R. Bloem, I. Toni, Pallidal dysfunction drives a cerebellothalamic circuit into Parkinson tremor. *Ann. Neurol.* **69**, 269–281 (2011).

57. V. A. Coenen, B. Sajonz, T. Prokop, M. Reisert, T. Piroth, H. Urbach, C. Jenkner, P. C. Reinacher, The dentato-rubro-thalamic tract as the potential common deep brain stimulation target for tremor of various origin: An observational case series. *Acta Neurochir. (Wien)* **18**, 130–114 (2020).

58. Y. Smith, M. D. Bevan, E. Shink, J. P. Bolam, Microcircuitry of the direct and indirect pathways of the basal ganglia. *Neuroscience* **86**, 353–387 (1998).

59. D. Plenz, S. T. Kital, A basal ganglia pacemaker formed by the subthalamic nucleus and external globus pallidus. *Nature* **400**, 677–682 (1999).

60. J. A. Obeso, M. C. Rodríguez-Oroz, M. Rodríguez, J. L. Lanciego, J. Artieda, N. Gonzalo, C. W. Olanow, Pathophysiology of the basal ganglia in Parkinson's disease. *Trends Neurosci.* **23**, S8–S19 (2000).

61. S. A. Wilson, The Croonian Lectures on some disorders of motility and of muscle tone, with special reference to the corpus striatum. *Lancet* **206**, 215–219 (1925).

62. C. D. Marsden, J. A. Obeso, The functions of the basal ganglia and the paradox of stereotaxic surgery in Parkinson's disease. *Brain* **117**, 877–897 (1994).

63. L. Alvarez, R. Macias, N. Pavón, G. López, M. C. Rodríguez-Oroz, R. Rodríguez, M. Alvarez, I. Pedroso, J. Teijeiro, R. Fernández, E. Casabona, S. Salazar, C. Maragoto, M. Carballo, I. García-Maeso, J. Guridi, J. L. Juncos, M. R. DeLong, J. A. Obeso, Therapeutic efficacy of unilateral subthalamotomy in Parkinson's disease: Results in 89 patients followed for up to 36 months. *J. Neurol. Neurosurg. Psychiatry* **80**, 979–985 (2009).

64. R. Rodriguez-Rojas, M. Carballo-Barreda, L. Alvarez, J. Guridi, N. Pavon, I. Garcia-Maeso, R. Macias, M. C. Rodriguez-Oroz, J. A. Obeso, Subthalamotomy for Parkinson's disease: Clinical outcome and topography of lesions. *J. Neurol. Neurosurg. Psychiatry* **89**, 572–578 (2018).

65. E. Brunner, U. Munzel, The nonparametric Behrens-Fisher problem: Asymptotic theory and a small-sample approximation. *Biom. J.* **42**, 17–25 (2000).

66. C. Rorden, L. Bonilha, T. E. Nichols, Rank-order versus mean based statistics for neuroimaging. *Neuroimage* **35**, 1531–1537 (2007).

67. T. A. Dembek, M. T. Barbe, M. Åström, V. Visser-Vandewalle, G. R. Fink, L. Timmermann, Probabilistic mapping of deep brain stimulation effects in essential tremor. *Neuroimage Clin.* **13**, 164–173 (2016).

68. M. Wintermark, J. Druzgal, D. S. Huss, M. A. Khaled, S. Monteith, P. Raghavan, T. Huerta, L. C. Schweickert, B. Burkholder, J. J. Loomba, E. Zadicario, Y. Qiao, B. Shah, J. Snell, M. Eames, R. Frysinger, N. Kassell, W. J. Elias, Imaging findings in MR imaging-guided focused ultrasound treatment for patients with essential tremor. *AJNR Am. J. Neuroradiol.* **35**, 891–896 (2014).

69. A. Klein, J. Andersson, B. A. Ardekani, J. Ashburner, B. Avants, M. C. Chiang, G. E. Christensen, D. L. Collins, J. Gee, P. Hellier, J. H. Song, M. Jenkinson, C. Lepage, D. Rueckert, P. Thompson, T. Vercauteren, R. P. Woods, J. J. Mann, R. V. Parsey, Evaluation of 14 nonlinear deformation algorithms applied to human brain MRI registration. *Neuroimage* **46**, 786–802 (2009).

70. Q. Wang, H. Akram, M. Muthuraman, G. Gonzalez-Escamilla, S. A. Sheth, S. Oxenford, F. C. Yeh, S. Groppa, N. Vanegas-Arroyave, L. Zrinzo, N. Li, A. Kühn, A. Horn, Normative vs. patient-specific brain connectivity in deep brain stimulation. *Neuroimage* **224**, 117307 (2021).

71. C. G. Goetz, B. C. Tilley, S. R. Shaftman, G. T. Stebbins, S. Fahn, P. Martinez-Martin, W. Poewe, C. Sampaio, M. B. Stern, R. Dodel, B. Dubois, R. Holloway, J. Jankovic, J. Kulisevsky, A. E. Lang, A. Lees, S. Leurgans, P. A. LeWitt, D. Nyenhuis, C. W. Olanow, O. Rascol, A. Schrag, J. A. Teresi, J. J. van Hilten, N. LaPelle, Movement Disorder Society UPDRS Revision Task Force, Movement Disorder Society-sponsored revision of the Unified Parkinson's Disease Rating Scale (MDS-UPDRS): Scale presentation and clinimetric testing results. *Mov. Disord.* **23**, 2129–2170 (2008).

72. J. Ashburner, A fast diffeomorphic image registration algorithm. *Neuroimage* **38**, 95–113 (2007).

73. T. A. Dembek, J. C. Baldermann, J. N. Petry-Schmelzer, H. Jergas, H. Treuer, V. Visser-Vandewalle, H. S. Dafsari, M. T. Barbe, Sweetspot mapping in deep brain stimulation: Strengths and limitations of current approaches. *Neuromodulation* **25**, 877–887 (2022).

74. J. Medina, D. Y. Kimberg, A. Chatterjee, H. Coslett, Inappropriate usage of the Brunner-Munzel test in recent voxel-based lesion-symptom mapping studies. *Neuropsychologia* **48**, 341–343 (2010).

75. Y. Iturria-Medina, E. J. Canales-Rodríguez, L. Melie-García, P. A. Valdés-Hernández, E. Martínez-Montes, Y. Alemán-Gómez, J. M. Sánchez-Bornot, Characterizing brain anatomical connections using diffusion weighted MRI and graph theory. *Neuroimage* **36**, 645–660 (2007).

76. B. L. Edlow, A. Mareyam, A. Horn, J. R. Polimeni, T. Witzel, M. D. Tisdall, J. C. Augustinack, J. P. Stockmann, B. R. Diamond, A. Stevens, L. S. Tirrell, R. D. Folkerth, L. L. Wald, B. Fischl, A. van der Kouwe, 7 Tesla MRI of the ex *vivo* human brain at 100 micron resolution. *Sci. Data* **6**, 244 (2019).

77. A. J. Rico, P. Barroso-Chinea, L. Conte-Perales, E. Roda, V. Gómez-Bautista, M. Gendive, J. A. Obeso, J. Lanciego, A direct projection from the subthalamic nucleus to the ventral thalamus in monkeys. *Neurobiol. Dis.* **39**, 381–392 (2010).

78. S. Ewert, P. Plettig, N. Li, M. M. Chakravarty, D. L. Collins, T. M. Herrington, A. A. Kühn, A. Horn, Toward defining deep brain stimulation targets in MNI space: A subcortical atlas based on multimodal MRI, histology and structural connectivity. *Neuroimage* **170**, 271–282 (2018).

79. G. Schaltenbrand, W. Wahren, *Atlas of Stereotaxy of the Human Brain* (Thieme, 1977).